

Learning Force-Regulated Manipulation with a Low-Cost Tactile-Force-Controlled Gripper

Xuhui Kang^{*1}, Tongxuan Tian^{*1}, Sung-Wook Lee¹, Binghao Huang², Yunzhu Li², Yen-Ling Kuo¹

Abstract—Successfully manipulating many everyday objects, such as potato chips, requires precise force regulation. Failure to modulate force can lead to task failure or irreversible damage to the objects. Humans can precisely achieve this by adapting force from tactile feedback, even within a short period of physical contact. We aim to give robots this capability. However, commercial grippers exhibit high cost or high minimum force, making them unsuitable for studying force-controlled policy learning with everyday force-sensitive objects. We introduce TF-Gripper, a low-cost (~\$150) force-controlled parallel-jaw gripper that integrates tactile sensing as feedback. It has an effective force range of 0.45–45 N and is compatible with different robot arms. Additionally, we designed a teleoperation device paired with TF-Gripper to record human-applied grasping forces. While we can train standard low-frequency policies with the collected force data, achieving reliable performance remains challenging due to the reactive and contact-dependent nature of force-regulated manipulation. To overcome this, we propose RETAF (REactive Tactile Adaptation of Force), a framework that decouples grasping force control from arm pose prediction. RETAF regulates force at high frequency using wrist images and tactile feedback, while a base policy predicts end-effector pose and gripper open/close action. We evaluate TF-Gripper and RETAF across five real-world tasks requiring precise force regulation. Our results show that, compared to position control, direct force control with TF-Gripper improves grasp stability and overall task performance. We further show that tactile feedback is essential for force regulation, and that RETAF consistently outperforms baselines and can be integrated with various base policies. We hope this work opens a path for scaling the learning of force-controlled policies in robotic manipulation. The project page is available at <https://force-gripper.github.io>.

I. INTRODUCTION

Humans have demonstrated strong capability in manipulating everyday objects that require precise force regulation, such as picking up potato chips or squeezing ketchup from bottles. We achieve this by adjusting forces from tactile feedback even within a short period of physical contact, see Fig. 1(a). With insufficient force, the task could not proceed, but excessive force could lead to irreversible object damage. However, existing works on robotic systems, with or without tactile feedback [1, 2], mostly simplify gripper control to binary open/close actions or direct gripper position/width prediction [3]–[10]. Such position control can be viewed as an indirect proxy for force control, as the manipulation goal is ultimately to apply an appropriate contact force. However, using position control to generate appropriate force is highly

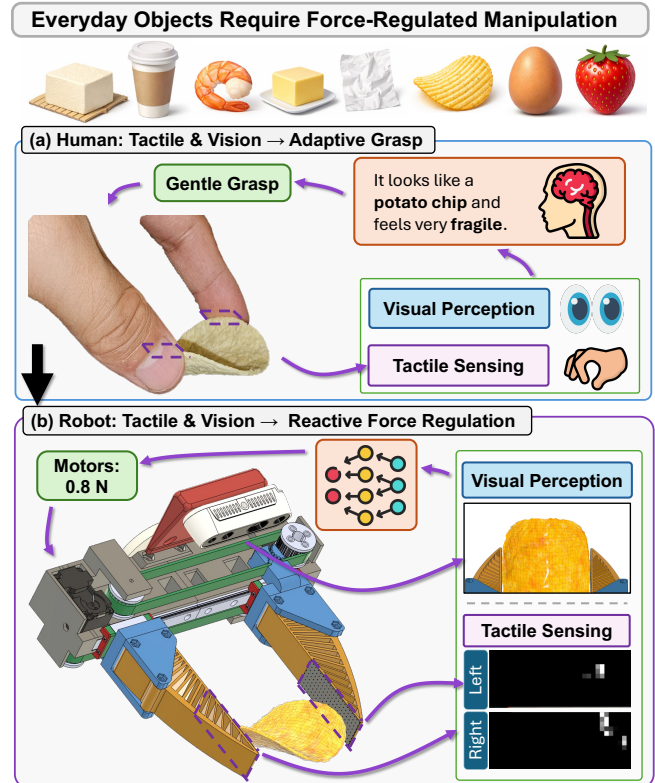


Fig. 1: To mimic the human ability to regulate force through tactile feedback to manipulate everyday objects, we develop a force-controlled gripper with tactile sensing for learning reactive and gentle manipulation policies.

object- and task-dependent. For example, in Fig. 2(a), a small variation in sizes can yield significant differences in stable grasping width range, whereas the stable grasping force range remains similar and can lead to more robust policies. In Fig. 2(b), on the other hand, the appearance is almost identical, but it requires a totally different width range to generate sufficient friction for a stable grasp. To successfully pick up the cherry tomato, the force control can easily adjust the force range from the tactile feedback, whereas position control will need to integrate information about the perceived tomato size and tactile input to infer the gripper width, which is harder to learn.

To study how the robot can effectively learn the human-like tactile-force capability, we need a gripper that supports force control. Many commercial grippers provide force control, but they are often expensive, difficult to adapt across different robots, and offer a high minimum force that is not

^{*}Equal contribution.

¹Department of Computer Science, University of Virginia, Charlottesville, VA, USA. {xuhui, nua3jz, ylkuo}@virginia.edu

²Department of Computer Science, Columbia University, New York, NY, USA. {binghao.huang, yunzhu.li}@columbia.edu

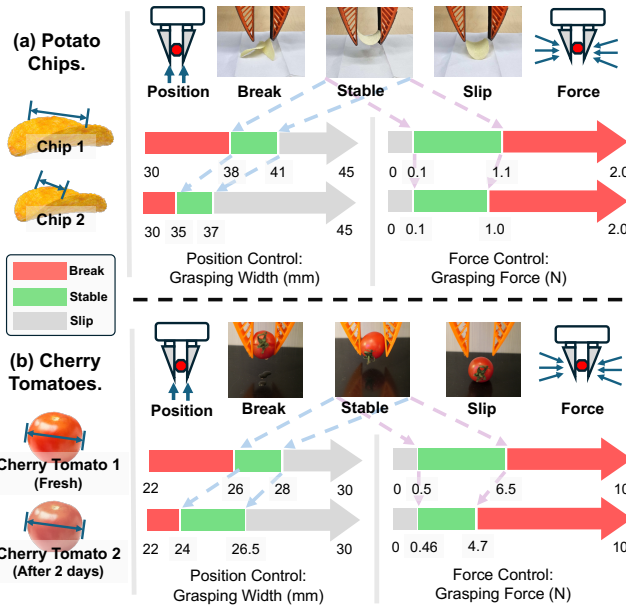


Fig. 2: Gripper position vs. force control on objects with similar appearance but different physical properties. (a) The same type of potato chips but with a small variation in size. (b) The same cherry tomato after two days of softening.

well suited for delicate, soft, and fragile everyday objects, as summarized in Tab. I. To enable more research in learning force-regulated manipulation, we develop and open-source TF-Gripper (Tactile-Force-Controlled Gripper), a universal and low-cost robotic gripper that provides fine-grained force regulation with tactile sensing, see Fig. 1(b). The TF-Gripper includes a teleoperation device that captures the force applied by a human operator through a spring-like actuator, which provides local kinesthetic feedback while estimating the applied force via motor current, and maps this signal to the gripper mounted on the robot during human demonstrations. This setting is sufficient to collect high-quality force control data, as the compliant interaction reduces variability while preserving fine-grained force modulation for learning force-regulated manipulation.

TABLE I: Mainstream Grippers with Force Control

Gripper	Cross-Robot Compatibility	Force Range (N)	Travel Range (mm)	Price
Franka Hand [11]	No	30–70	80	~\$2,000
Robotiq 2F-85 [12]	Yes	25–235	85	~\$5,000
xArm Gripper G2 [13]	No	10–50	84	~\$2,200
WSG-50 [14]	Yes	5–80	110	~\$5,600
OnRobot RG2 [15]	Yes	3–40	110	~\$5,500
Flexiv Grav [16]	No	1–100	100	~\$6,000
TF-Gripper (Ours)	Yes	0.45–45	95	~\$150

It is possible to train a force control policy using the existing model architecture like diffusion policy (DP) [17] or vision-language-action (VLA) models [18, 19]. These models jointly predict the robot arm pose and gripper command (mostly, gripper width in prior works) at a relatively low frequency (e.g., 1–10 Hz). However, force control introduces

a fundamentally different control objective from position control. Rather than reaching a gripper position, the gripper closes by continuously applying a specified force, and success depends on how that force is regulated during a short, contact-rich interaction phase. A low-frequency policy is insufficient to capture fine-grained contact dynamics and thus struggles to support force-regulated manipulation which requires fast, contact-driven adaptation. Moreover, directly fusing tactile inputs with global visual observations can confuse the policy and often leads to unstable learning [6, 20].

To address these issues, we propose **RETAF** (REactive Tactile Adaptation of Force), a policy design that explicitly decouples arm pose prediction from grasping force prediction. RETAF employs a force adaptation policy to reactively predict force at a high frequency (30 Hz) based on wrist-view images and tactile feedback, while a base policy predicts end-effector pose and gripper open/close actions. This design enables rapid force adaptation during contact and only considers tactile information when needed. We evaluate TF-Gripper and RETAF with five real-world manipulation tasks that require precise force regulation to complete. We collected 50 human demonstrations for each task using the TF-Gripper. Experimental results show that RETAF can be integrated with different pose prediction policies and consistently improves grasp stability, pose execution quality, and overall task success in force-regulated manipulation.

In summary, our work makes the following contributions:

- 1) We introduce TF-Gripper, a low-cost (~\$150) tactile-force-controlled gripper, enabling precise force control (0.45–45 N) during contact. It pairs with a teleoperation device for collecting demonstrations with force control.
- 2) We propose RETAF, a policy framework that decouples force control from end-effector pose prediction and can be integrated with any existing pose-prediction policies.
- 3) We evaluate the TF-Gripper and RETAF with real-world force-regulated manipulation tasks, showing the improved performance over pose control and the effectiveness in reactive force regulation.

II. RELATED WORK

Force-Controlled Grippers. Force-controlled grippers regulate the contact force applied to objects to enable compliant interactions. Existing designs can be categorized into open-loop and closed-loop approaches. Open-loop force control estimates grasping force indirectly, typically via motor current or actuator torque, and is widely used in commercial and open-source grippers. Commercial systems, e.g., Robotiq 2F-85 [12] and WSG-50 [14], rely on actuator current for force estimation, but often struggle to achieve precise low-force regulation. Open-source designs like MAGPIE [21] also uses actuator current; however, backlash and position-dependent moment arms make consistent force control difficult. Closed-loop force control improves accuracy by incorporating direct force or contact feedback. For example, WSG-50 and ECHO [22] support an fingertip-mounted torque sensor. Learning-based approaches such as FARM [23] estimate

contact force from tactile observations for closed-loop control. Despite improved precision, these approaches depend on specialized fingertips or additional sensors, which limits compatibility with general-purpose [24] or task-customized fingertips [25] commonly used in learning-based manipulation. In contrast, our gripper employs a timing-belt transmission to minimize backlash and maintain a consistent moment arm, enabling precise open-loop force regulation without expensive torque sensors, while natively integrating tactile sensing to support learning-based closed-loop adaptation.

Force-Aware Teleoperation and Data Collection. A key challenge in learning force-regulated manipulation is capturing the grasping force applied by human operators during demonstrations. Existing teleoperation frameworks [26, 27] and data collection systems [24] mainly focus on end-effector pose and gripper open/close or width, but do not support human-applied grasping force. Recent works attempt to infer force indirectly, for example, by estimating intended force from joystick signals and motor feedback [22], or by predicting contact forces from tactile observations during manipulation [28]. However, these approaches do not directly capture the force input applied by the human operator. FTF [29] measures 3D contact forces using a tactile glove, but targets natural human manipulation rather than robot teleoperation. UMI-FT [30] collects in-the-wild contact force data by augmenting the gripper with a force sensor. In contrast, we design a teleoperation device that directly measures the force applied by the human operator and maps it to the robot gripper in real time. This enables the direct recording of ground-truth human grasping force, eliminating the need for indirect inference from proxy signals (e.g., joystick position) or offline post-hoc estimation. Moreover, our device is independent of the pose teleoperation interface and can be combined with VR controllers, SpaceMouse, or other pose input devices, providing a more direct and flexible solution for collecting force-aware manipulation data.

Learning with Force and Tactile. Tactile sensing has been widely used in learning-based manipulation to improve contact awareness and robustness. Most prior work focuses on how to encode tactile information or integrate it into policy architectures for contact-rich interactions [31], such as reactive control [20], sim-to-real refinement [32], or multimodal representation learning [3]. However, these approaches primarily treat tactile feedback as an auxiliary observation and do not explicitly study tactile-driven force control. Several works begin to address grasping force learning. FARM [28] estimates object–gripper contact force distributions from tactile observations and provides them as inputs to a manipulation policy. More recently, Kuo et al. [33] propose a physics-informed energy-based abstraction to learn slip-aware grasping force control from tactile sensing. In contrast, our work focuses on learning reactive grasping force control for force-regulated manipulation by explicitly decoupling force control from pose prediction. We leverage tactile feedback to drive a force adaptation policy that operates at high frequency, enabling precise and adaptive force regulation during contact.

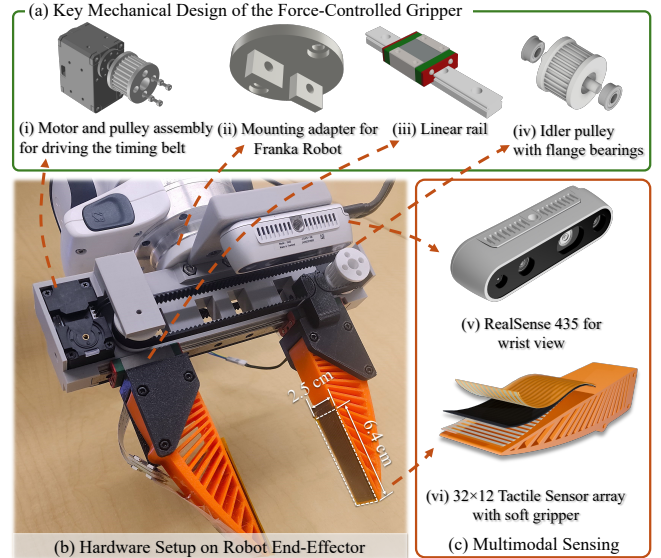


Fig. 3: Hardware design of the TF-Gripper. (a) Key components: An adapter connects the gripper to a robot and two motors actuate the fingertips along linear rails by pulling a timing belt. (b) The overall TF-Gripper setup, with the main structure fully 3D printed. (c) A camera provides a wrist view, with soft fingertips integrated with tactile sensors.

III. TF-GRIPPER HARDWARE SYSTEM DESIGN

A. Gripper Design

To enable precise, low-cost force control for force-regulated manipulation, we develop a compact parallel-jaw gripper **TF-Gripper** (Tactile-Force-Controlled gripper) driven by two Dynamixel XL430-W250-T [34] actuators. Fig. 3 illustrates the overall hardware design. The gripper adopts a pulley-and-timing-belt transmission mechanism (Fig. 3 (b)). Each motor drives a pulley that pulls a timing belt to actuate one fingertip, where the effective moment arm is determined by the pulley radius (Fig. 3 (i)). This transmission provides a reliable and repeatable mapping from motor torque to fingertip force while maintaining mechanical robustness. The main gripper frame is fully 3D printed. Each fingertip is mounted on a linear slider that moves along a low-friction linear rail, ensuring stable and smooth parallel motion during grasping (Fig. 3 (iii)). On the passive side, the timing belt is routed through an idler pulley composed of a cylindrical shaft and two flanged bearings, which further reduces friction and improves motion consistency (Fig. 3 (iv)). To support compliant contact with objects, the fingertips are equipped with soft fingertip pads from UMI [24] (Fig. 3 (vi)). To further enable reliable tactile perception at low cost, we integrate thin and soft piezo-resistive tactile sensors, *FlexiTac* [2, 3], which capture both contact area geometry and force-related information while maintaining mechanical softness. The gripper is mounted on the robot via an interchangeable adapter. For robots such as the Franka Research 3 and UR5, we provide an ISO 9409-1-A50 compatible adapter (Fig. 3 (ii)). For robots following

other mounting standards, e.g., KUKA KR10 R1100, only the adapter needs to be replaced.

The Dynamixel actuators exhibit a near-linear current-to-force relationship when evaluated 1 cm from the end of the fingertip. This enables accurate and stable force control over a range of approximately 0.4–45 N, with a resolution of about 0.2 N. This relationship is empirically validated in

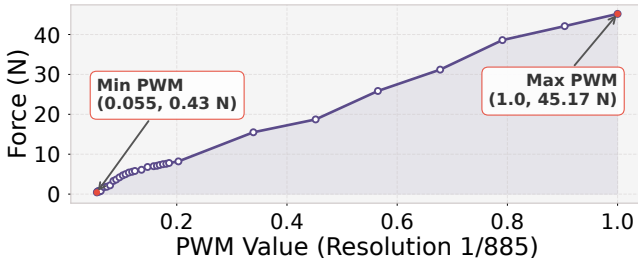


Fig. 4: Actuator current (PWM)–force relationship. The force is measured at the fingertip contact surface, reflecting the effective grasping force applied by the TF-Gripper.

Fig. 4, which shows a consistent and monotonic mapping between the actuator current (PWM) and the measured fingertip force. We further evaluate force stability under temperature variations. After running the actuator at 20% current for 20 minutes at 25 °C, we observe an average force drift of about 9%. Using the motor’s built-in temperature sensor for compensation reduces this error to below 4%, indicating stable force control over extended operation.

B. Teleoperation Device

Most existing teleoperation methods, such as VR controllers, SpaceMouse devices, or kinesthetic teaching, primarily focus on joints or end-effector pose control. In these systems, gripper commands are typically limited to discrete open/close actions or continuous position control, making it difficult to capture human-applied grasping force. To collect human demonstrations with explicit force control for policy training, we design a low-cost teleoperation interface (<\$100) that mirrors the gripper’s actuation mechanism.

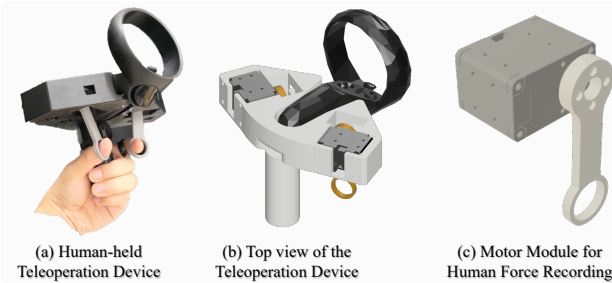


Fig. 5: Design of the teleoperation device. A VR controller controls the robot’s end-effector pose. Two figure rings are connected to the motors; they detect the force applied by the human operator to drive the TF-Gripper.

As shown in Fig. 5, our teleoperation device has a VR controller mounted for controlling the robot’s end-effector

pose and two finger rings for humans to input grasping force. The finger rings are connected to the same Dynamixel actuator as in the gripper. The actuator is configured to provide spring-like resistance, offering local kinesthetic feedback while measuring the operator’s applied force via motor current. This signal is calibrated and mapped to the current command of the robot gripper actuator, allowing the robot to reproduce the demonstrated gripping force in real time.

IV. RETAF: REACTIVE TACTILE ADAPTATION OF FORCE

A. Problem Formulation

We formulate a manipulation task as a sensorimotor problem. At time t , observation is $o_t = \{V_t, \mathcal{T}_t\}$, where V_t represents general non-tactile observations (e.g., RGB images, proprioception) and \mathcal{T}_t represents tactile readings. The goal is to learn a control policy π that maps these observations to an action a_t . The traditional action space a_t consists of the robot arm command a_t^{pose} (e.g., end-effector pose) and the gripper command a_t^{grip} (typically position width): $a_t = [a_t^{\text{pose}}, a_t^{\text{grip}}] \sim \pi(V_t, \mathcal{T}_t)$. However, this coupled formulation of predicted actions introduces two fundamental mismatches for force-regulated manipulation: **1) Frequency Mismatch.** Stable force regulation relies on reacting to transient tactile events (e.g., slip) within a short reaction time (e.g., $\tau_{\text{react}} \leq 50$ ms). In contrast, pose prediction a_t^{pose} typically employs large backbones with a higher inference latency (typically $100 \text{ ms} < \tau_{\text{lat}} < 1000$ ms). A coupled policy is bottlenecked by this slow inference ($\tau_{\text{lat}} \gg \tau_{\text{react}}$), making force control to be insufficiently reactive to contact dynamics. **2) Learning with Tactile.** Integrating tactile feedback into the policy is non-trivial. Tactile signals \mathcal{T}_t are sparse and highly contact-dependent, whereas visual observations V_t are dense and globally structured. Directly fusing these modalities often leads to unstable learning or optimization difficulties, as the policy struggles to weigh the local, transient tactile signal against the dominant global visual context [6, 20].

B. The RETAF Framework

To address these challenges, we decouple the policy into two components: a Base Policy π_{base} for trajectory generation and a Force Adaptation Policy π_{force} for contact regulation, see Fig. 6. The force policy is activated by a discrete gripper action $k_t \in \{\text{open}, \text{close}\}$ predicted by the base policy.

Base Policy (π_{base}). We leverage existing visuomotor policy architectures as the base policy without architectural modifications for tactile fusion. Operating at low frequency, π_{base} predicts the arm pose and the discrete gripper open/close using non-tactile observations: $(a_t^{\text{pose}}, k_t) = \pi_{\text{base}}(V_t)$. We train π_{base} via behavior cloning to match the expert actions $a_t^* = (a_t^{\text{pose}*}, k_t^*)$. The objective is to minimize the loss \mathcal{L} between the predicted policy and the ground truth:

$$\mathcal{L}_{\text{base}} = \mathbb{E}_{(V_t, a_t^*) \sim \mathcal{D}} [\mathcal{L}(\pi_{\text{base}}(V_t), a_t^*)] \quad (1)$$

where \mathcal{L} is the architecture-specific loss function (e.g., MSE noise prediction loss for Diffusion Policy).

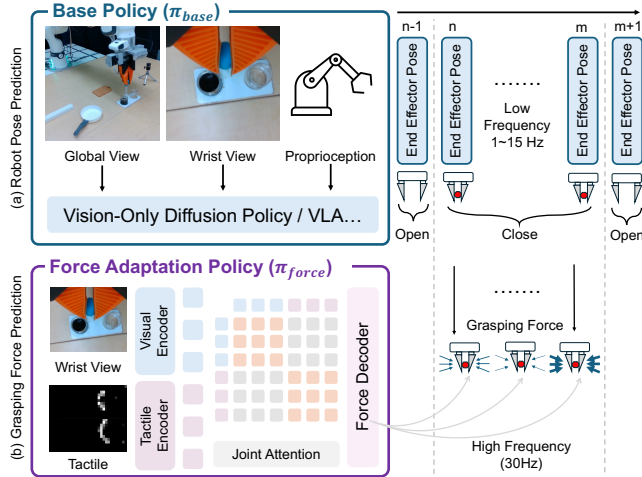


Fig. 6: Overview of the RETAF framework. The base policy predicts end-effector pose and gripper open/close from visual and proprioceptive observations at a low frequency. When the gripper closes, the force adaptation policy is activated to predict grasping force at a high frequency using joint attention over wrist-view and tactile inputs.

Force Adaptation Policy (π_{force}). The final gripper action a_t^{grip} is determined by the trigger k_t . The π_{force} is activated *only* when the base policy signals a grasp intent ($k_t = \text{close}$):

$$a_t^{\text{grip}} = \begin{cases} \pi_{\text{force}}(I_t^{\text{wrist}}, \mathcal{T}_t) & \text{if } k_t = \text{close} \\ \emptyset (\text{Open}) & \text{if } k_t = \text{open} \end{cases} \quad (2)$$

When activated, π_{force} predicts the continuous target force f_t at high frequency ($>30\text{ Hz}$). Since the force adaptation policy only needs to reason about grasping force, we design it to attend exclusively to wrist-view visual observations (I_t^{wrist}) and tactile sensing (\mathcal{T}_t) through a joint-attention layer [35]. The wrist view provides compact, object-centric visual information, including object category, shape, and surface appearance, while tactile sensing provides local feedback, capturing signals such as deformation and incipient slip. By jointly attending to these two complementary modalities, RETAF enables precise and stable force control without being distracted by irrelevant information from the global scene. We train π_{force} via supervised regression to match the demonstrator's applied force f_t^* . The objective is to minimize the mean squared error (MSE):

$$\mathcal{L}_{\text{force}} = \mathbb{E}_{(I_t^{\text{wrist}}, \mathcal{T}_t, f_t^*) \sim \mathcal{D}} [\|\pi_{\text{force}}(I_t^{\text{wrist}}, \mathcal{T}_t) - f_t^*\|^2] \quad (3)$$

This lightweight design allows inference at 80 Hz+ on a single RTX 5070 Ti, satisfying the frequency requirements for reactive force regulation.

V. EXPERIMENTAL SETUP

We conduct real-world experiments on tasks that require precise force-regulation to evaluate TF-Gripper and RETAF.

A. Hardware and Data Collection

Hardware Setup. Our experimental platform consists of a Franka Research 3 robot equipped with the proposed TF-Gripper. Two Intel RealSense D435i cameras are used: one is placed in a third-person view to capture the global scene, and another is mounted on the gripper to provide wrist-view visual observations. All experiments are conducted on a tabletop setup, as in Fig. 7, containing everyday objects including a plate, a bowl, a pan, a cup, and a dropper.

Data Collection. Data is collected using our custom teleoperation device (Fig. 5) where a Meta Quest 1 is employed as the mounted VR controller. During teleoperation, we record the full robot trajectory at 15 Hz , including end-effector pose, gripper force, gripper positions, as well as visual and tactile observations. For each task, we collect 50 human demonstrations, with each trajectory lasting for 4 to 10 seconds based on the tasks. This data collection setup allows us to obtain demonstrations that explicitly encode force changes during manipulation. We can directly compare position control with force control under identical task conditions and evaluate their effectiveness in force-regulated manipulation tasks.

B. Baselines

We compare RETAF against two representative learning-based manipulation baselines.

Diffusion Policy [17] (DP) is one of the most widely adopted policies for robot manipulation and has demonstrated strong performance across many tasks. It predicts action sequences by iteratively denoising random noise and serves as a strong baseline. We evaluate DP variants with and without tactile input, and with gripper actions represented as either gripper position or grasping force.

ViTac-MAE [3] extends DP by pretraining a tactile encoder using masked autoencoding, resulting in improved tactile representations. By comparing ViTac-MAE with standard DP under identical settings, we examine whether a stronger tactile representation alone is sufficient to address the challenges of learning precise force control.

C. Implementation Details

Across all methods, the action space consists of the absolute end-effector position, absolute end-effector rotation represented using a 6D rotation representation [36], and a gripper action. Depending on the method, the gripper action can be either open/close, continuous gripper position, or continuous grasping force. For visual observations, RGB images are encoded using the image encoder from CLIP [37]. Tactile observations are encoded using a two-layer convolutional neural network. All DP and ViTac-MAE variants use a 1D U-Net as the diffusion backbone. For RETAF, the base policy adopts the same DP architecture to predict only end-effector pose and a binary gripper open/close action using visual observations. When the gripper closes, the force adaptation policy is activated and predicts the target grasping force

from wrist-view images and tactile feedback. In position-based control experiments, the same force adaptation policy architecture is employed to predict gripper position.

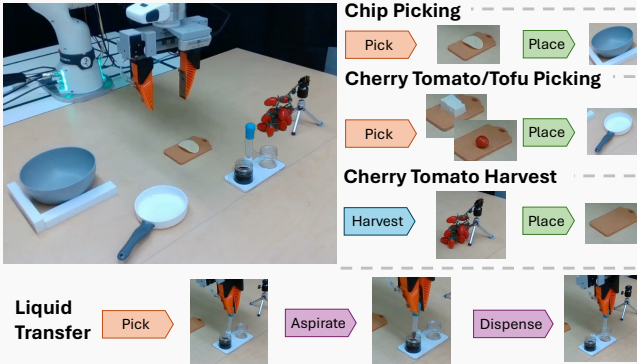


Fig. 7: Overview of the evaluation environment, illustrating how each task is performed in this setup.

D. Tasks Setup

We designed five manipulation tasks, as shown in Fig. 7, that require continuous and precise grasping force control. In all tasks, excessive force or overly small gripper width risks breaking objects, while insufficient force or overly wide gripper width leads to slippage or failure to lift. We define each task and its stable grasp below.

- 1) **Tofu Grasping:** The robot grasps and transfers soft tofu cubes with edge ranging from 2 to 5 cm. Depending on the cube size and firmness, stable grasp typically requires force between 2 and 5 N. *Stable grasp:* deformation < 20% and no breakage.
- 2) **Chip Picking:** Pick a potato chip from a board and places it into a bowl. The chips are from the same brand and appear to be visually similar, but require different gripper positions or force to manipulate successfully. In addition, chips may be placed in either orientation (front or back). Chips are highly fragile and can break with a minimum force at about 1.5 N. *Stable grasp:* lifting without damage.
- 3) **Cherry Tomato Picking:** The robot picks up a real cherry tomato from a board and places it into a bowl. Cherry tomatoes typically have diameters of 2–3 cm, but exhibit large variations in softness due to ripeness. A successful grasping requires force control over a wide range, from about 0.5 to 7 N. *Stable grasp:* deformation < 20%.
- 4) **Liquid Transfer:** The robot grasps a dropper, draws liquid from a cup, and dispenses it into an empty cup. As liquid is drawn into or expelled from the dropper, the dropper's effective weight and internal pressure change. A stable grasp therefore requires continuous force adjustment, typically within the range of 0.8 to 3 N, to support both suction and squeezing actions. *Stable grasp:* no spilling and no dropper drop during transfer.
- 5) **Cherry Tomato Harvest:** The robot plucks a cherry tomato from an artificial vine, which is used to ensure repeatability. Although tomatoes on the same vine appear

visually similar, different attachment positions require adaptive forces (2 to 5 N) to generate sufficient friction during pulling without slipping and damaging them. *Stable grasp:* deformation < 20%.

E. Evaluation Metrics

We evaluate each task with 10 rollouts. Fig. 9(a) shows an example rollout for the Tofu Grasping task. To better understand where and why a policy fails, we do not rely solely on the overall task success rate. Instead, we decompose each task into three stages to report the average success rate.

Reach measures whether the robot can successfully move to the target object and make contact with it. This stage is a prerequisite for manipulating objects.

Stable Grasp evaluates whether the object can be held stably after grasping and throughout task execution, without slipping, dropping, excessive deformation, or damage.

Task Success measures whether the robot can complete the full task such as placing, transferring, or releasing the object as required.

VI. EXPERIMENT RESULTS

We investigate four key research questions:

- 1) **RQ1.** Does direct force control improve force-sensitive tasks compared to position control?
- 2) **RQ2.** Is tactile sensing necessary for precise and effective force control?
- 3) **RQ3.** Does RETAF improve force-sensitive tasks compared to non-reactive baselines?
- 4) **RQ4.** How well can RETAF be integrated with different base policies?

A. Force Control vs. Position Control (RQ1)

We compare force-based and position-based gripper control across all five tasks. Table II shows that force control consistently achieves higher stable grasp rates than position control across different policies, while keeping the performance of the reach stage performance similar or only slightly lower. For DP and ViTac-MAE baselines, switching from position to force control also leads to improvements in grasp stability. For example, DP improves its stable grasp rate from 28% to 38%, and ViTac-MAE from 32% to 40%. This trend becomes more pronounced when combined with RETAF. RETAF with force control achieves a stable grasp rate of 68%, compared to 44% under position control. These results indicate that the advantage of force control arises during physical contact rather than object reaching.

B. The Role of Tactile Sensing (RQ2)

As shown in Table II, adding tactile input to DP leads to only small improvements in stable grasp rates compared to the DP without tactile sensing, indicating that directly fusing tactile observations is not sufficient for effective force regulation. ViTac-MAE achieves better performance by learning stronger tactile representations, resulting in higher grasp stability and task success rate, but its overall improvement remains limited. In contrast, RETAF explicitly leverages

TABLE II: Performance in three stages, Reach (R), Stable Grasp (G), and Task Success (S), across five manipulation tasks.

Tasks		Cherry Tomato Picking			Tofu Grasping			Chip picking			Cherry Tomato Harvest			Liquid Transfer			Average		
Policy	Gripper Action	R	G	S	R	G	S	R	G	S	R	G	S	R	G	S	R	G	S
DP w/o Tac	Position Force	90% 80%	30% 40%	20% 30%	80% 60%	40% 40%	20% 20%	80% 70%	20% 30%	0% 0%	30% 20%	10% 20%	0% 0%	40% 40%	20% 30%	10% 10%	64% 54%	24% 32%	10% 12%
DP w/ Tac	Position Force	90% 90%	40% 40%	20% 30%	70% 80%	30% 50%	20% 40%	70% 70%	20% 30%	10% 10%	30% 30%	20% 20%	0% 0%	40% 50%	30% 40%	20% 20%	60% 64%	28% 38%	14% 20%
ViTac-MAE	Position Force	90% 90%	60% 60%	40% 50%	100% 80%	40% 50%	40% 50%	80% 70%	20% 20%	0% 10%	30% 30%	10% 20%	0% 10%	40% 50%	30% 50%	20% 30%	68% 64%	32% 40%	20% 30%
RETAFF (Ours)	Position Force	100% 100%	60% 90%	50% 80%	100% 100%	50% 90%	30% 80%	90% 90%	30% 50%	20% 40%	40% 50%	30% 40%	10% 30%	70% 70%	50% 60%	10% 10%	80% 60%	44% 68%	28% 60%

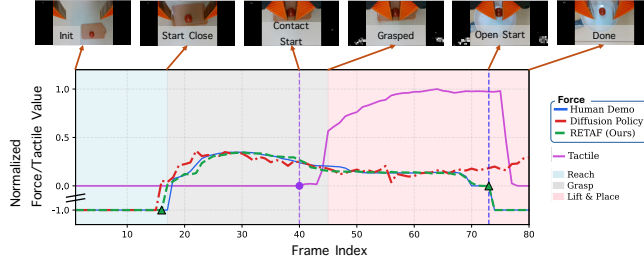


Fig. 8: Force prediction over time on a validation human demonstration: per frame, we compare Diffusion Policy (DP/Force) and RETAF predictions against ground-truth (Human Demo) force. We also plot tactile values (sum of tactile readings, scaled to [0, 1]) and force readings scaled to [-1, +1], where -1 denotes a predefined gripper-open action, and positive values indicate human-applied grasping force. RETAF tracks the ground-truth force more closely and captures the correct open timing, while DP/Force fails to predict the needed force accurately.

tactile feedback for reactive force adjustment and achieves consistent improvements across all stages over all baselines.

Fig. 8 provides an example of a validation human demonstration, comparing force predictions from DP and RETAF against the ground-truth human-applied force. After reaching the target pose, the human applies a larger force to close the gripper, and then adjusts the force upon contact based on tactile and visual feedback. Notably, the visual appearance before and after contact changes only subtly, making it difficult to infer the required grasping force from vision alone. Together, these results show that tactile sensing is essential for force-regulated manipulation, and that the way tactile information is used plays a critical role in performance.

C. Effectiveness of RETAF (RQ3)

Results in Table II show that RETAF consistently improves overall performance across all five tasks. RETAF outperforms both the DP and ViTac-MAE baselines in all stages. Notably, RETAF also leads to a higher success rate in the reach stage. Although both DP and RETAF are based on diffusion policies, restricting the gripper action to predicting only open/close, rather than force or position, simplifies policy learning and results in more accurate and reliable pose

prediction. As a result, the robot reaches target objects more consistently. In addition, RETAF leverages tactile feedback to adjust grasping force in a reactive manner, leading to significantly higher stable grasp rates. By combining improved pose prediction with effective force regulation during contact, this architecture enhances both reach and grasp stability, which ultimately lead to large gains in task success.

TABLE III: Quantitative results of RETAF when pairing with different base policies. Tasks are evaluated in three stages: Reach (R), Stable Grasp (G), and Task Success (S).

Base Policy	With RETAF?	Cherry Tomato Picking			Transfer Liquid		
		R	G	S	R	G	S
$\pi_{0.5}$	No	80%	30%	20%	60%	20%	20%
	Yes	100%	90%	90%	70%	60%	50%
DP	No	90%	50%	30%	50%	40%	20%
	Yes	100%	90%	80%	70%	60%	60%

D. RETAF with Different Base Policies (RQ4)

We evaluate the effectiveness of RETAF with different base policies on two representative tasks: Cherry Tomato Picking and Liquid Transfer. We employ $\pi_{0.5}$ and DP as candidate base policies. Without RETAF, the $\pi_{0.5}$ takes tactile input as an image to the VLA, and DP directly fuses tactile and visual observations as in previous experiments. As shown in Table III, RETAF consistently improves reach, stable grasp, and task success across both policies. For $\pi_{0.5}$ without RETAF, predicting grasping force leads to limited improvement in grasp stability, whereas using RETAF results in better overall performance. By offloading force regulation to RETAF, $\pi_{0.5}$ achieves large improvements in stable grasp rate, demonstrating that RETAF is effective even for a different base policy.

E. Qualitative Examples

Fig. 9(a) provides two qualitative rollout examples of RETAF where RETAF correctly predicts appropriate forces and achieves stable grasps. Fig. 9(b) illustrates common failure cases. During the reach-to-target stage, DP that predicts positions or forces exhibits a higher failure rate than DP predicting open/close actions; however, predicting open/close does not eliminate failures. In some cases, the grasp succeeds, but the task still fails due to incorrect pose

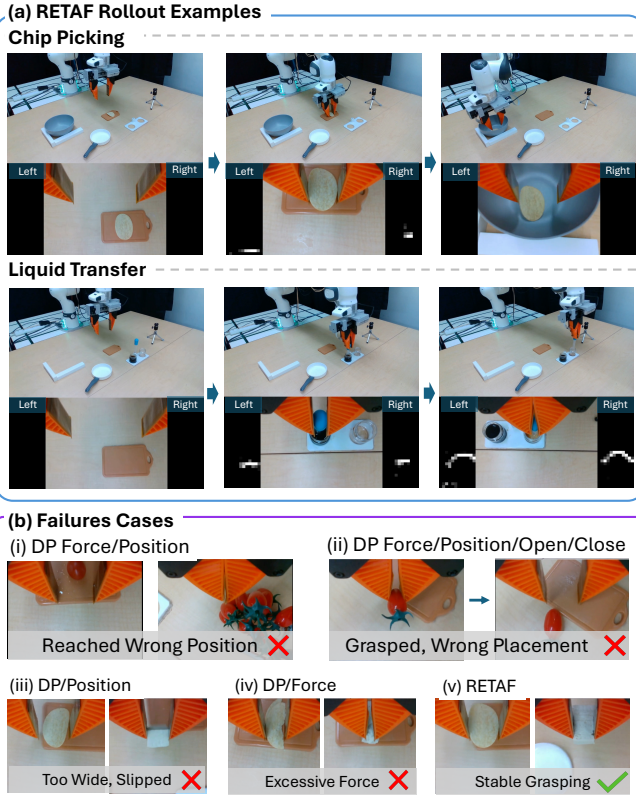


Fig. 9: (a) Two successful rollouts, where RETAF correctly predicts appropriate forces and achieves stable grasps. (b) Failure cases: (i) DP predicts force or width, it shows a higher failure rate during the reach-to-target stage than DP predicting open/close actions. (ii) Regardless of the gripper action type, DP often fails to predict accurate end-effector poses. (iii) We observe that DP-width tends to predict overly large widths, causing slip, while (iv) DP-force tends to predict excessive force, leading to object breakage. In contrast, (v) RETAF predicts more appropriate grasping forces.

predictions by DP. During grasping, we observe that DP predicting position tends to result in insufficient contact and slipping, consistent with our earlier analysis that position control is less robust to small variations in object width and can cause the policy to assume contact falsely. In contrast, DP with direct force prediction tends to output excessive forces. Force control can tolerate slightly smaller forces while still achieving task success, consistent with our earlier analysis of its robustness. However, without timely reactions to tactile feedback, DP often overestimates the required force. Overall, RETAF predicts more accurate and well-regulated grasping forces.

VII. CONCLUSION AND FUTURE WORK

In this work, we investigate how explicit force control with tactile feedback influences learning-based manipulation of force-sensitive everyday objects. To study this, we develop TF-Gripper with a teleoperation device for data collection, and RETAF, a policy framework that decouples force regula-

tion from pose prediction. Experiments across five real-world tasks demonstrate that force control consistently outperforms position control in grasp stability, and that RETAF further improves task performance across different base policies.

The evaluations presented in this work are empirical and can be limited by our selected tasks. In the future, understanding the theoretical effects of force- versus position-based control on learning, extending the analysis to a broader range of objects, and scaling force-regulated manipulation through large-scale force and tactile data collection could provide deeper insights into the design of robust policies for force-regulated manipulation.

ACKNOWLEDGMENTS

This work was partly supported by Delta Electronics Inc. We acknowledge Research Computing at the University of Virginia for providing the computational resources that made the results in this work possible.

REFERENCES

- [1] GelSight, Inc., “GelSight Mini,” https://www.gelsight.com/wp-content/uploads/2022/09/GelSight_Datasheet_GSMini_9.20.22b.pdf, 2022, version 9.20.22b.
- [2] B. Huang, Y. Wang, *et al.*, “3D ViTac: learning fine-grained manipulation with visuo-tactile sensing,” in *Conference on Robot Learning*, 2024.
- [3] X. Zhu, B. Huang, *et al.*, “Touch in the wild: Learning fine-grained manipulation with a portable visuo-tactile gripper,” *arXiv:2507.15062*, 2025.
- [4] Y. Xu, L. Wei, *et al.*, “exumi: Extensible robot teaching system with action-aware task-agnostic tactile representation,” in *Conference on Robot Learning*, 2025.
- [5] F. Liu, C. Li, *et al.*, “Vitamin: Learning contact-rich tasks through robot-free visuo-tactile manipulation interface,” *preprint arXiv:2504.06156*, 2025.
- [6] O. Mees, L. Hermann, *et al.*, “CALVIN: A benchmark for language-conditioned policy learning for long-horizon robot manipulation tasks,” *IEEE Robotics and Automation Letters (RA-L)*, 2022.
- [7] L. Wu, C. Yu, *et al.*, “Freetacman: Robot-free visuo-tactile data collection system for contact-rich manipulation,” *preprint arXiv:2506.01941*, 2025.
- [8] H.-S. Fang, H. Fang, *et al.*, “RH20T: A comprehensive robotic dataset for learning diverse skills in one-shot,” in *2024 IEEE International Conference on Robotics and Automation (ICRA)*, 2024.
- [9] Y. Mo, H. Zhang, *et al.*, “Towards open-world interactive disambiguation for robotic grasping,” in *IEEE International Conference on Robotics and Automation*, 2023.
- [10] E. Zhao, V. Raval, *et al.*, “ManipBench: Benchmarking vision-language models for low-level robot manipulation,” in *Conference on Robot Learning*, 2025.
- [11] Franka Emika, “Product manual: Franka hand,” https://download.franka.de/documents/220010_Product%20Manual_Franka%20Hand.1.2.EN.pdf, 2020, version 1.2, Document No. 220010.
- [12] Robotiq Inc., “2F-85 and 2F-140 instruction manual for e-series,” https://assets.robotiq.com/website-assets/support_documents/document/2F-85.2F-140_Instruction_Manual_e-Series.PDF_20190206.pdf, 2019, [Accessed: 01-20-2025].
- [13] “xArm Gripper,” <https://www.ufactory.us/product/ufactory-xarm-gripper>, [Accessed 27-12-2025].
- [14] “WSG-50,” <https://weiss-robotics.com/servo-electric/wsg-series/product/wsg/>, [Accessed 27-12-2025].
- [15] OnRobot, “RG2 Adaptive Gripper,” 2019, datasheet v1.4, available at <https://onrobot.com/en/products/rг2-finger-gripper>.
- [16] “Flexiv Grav,” <https://www.flexiv.com/products/grav>, [Accessed 27-12-2025].
- [17] C. Chi, Z. Xu, *et al.*, “Diffusion policy: Visuomotor policy learning via action diffusion,” *The International Journal of Robotics Research*, 2023.

- [18] M. Kim, K. Pertsch, *et al.*, “OpenVLA: An open-source vision-language-action model,” in *Conference on Robot Learning*, 2024.
- [19] K. Black, N. Brown, *et al.*, “π0: A vision-language-action flow model for general robot control,” *arXiv:2410.24164*, 2024.
- [20] H. Xue, J. Ren, *et al.*, “Reactive diffusion policy: Slow-fast visual-tactile policy learning for contact-rich manipulation,” in *Robotics: Science and Systems*, 2025.
- [21] N. Correll, D. Kriegman, *et al.*, “A versatile robotic hand with 3D perception, force sensing for autonomous manipulation,” in *RSS Workshop on Perception and Manipulation Challenges for Warehouse Automation*, 2023.
- [22] A. Bazhenov, S. Satsevich, *et al.*, “Echo: An open-source, low-cost teleoperation system with force feedback for dataset collection in robot learning,” *preprint arXiv:2504.07939*, 2025.
- [23] E. Helmut, N. Funk, *et al.*, “Tactile-conditioned diffusion policy for force-aware robotic manipulation,” *preprint arXiv:2510.13324*, 2025.
- [24] C. Chi, Z. Xu, *et al.*, “Universal manipulation interface: In-the-wild robot teaching without in-the-wild robots,” in *Robotics: Science and Systems*, 2024.
- [25] H. Ha, S. Agrawal, *et al.*, “Fit2Form: 3D generative model for robot gripper form design,” in *Conference on Robot Learning*, 2021.
- [26] A. Iyer, Z. Peng, *et al.*, “OPEN TEACH: A versatile teleoperation system for robotic manipulation,” in *Conference on Robot Learning*, 2025.
- [27] Z. Fu, T. Z. Zhao, *et al.*, “Mobile ALOHA: Learning bimanual mobile manipulation with low-cost whole-body teleoperation,” in *Conference on Robot Learning*, 2024.
- [28] E. Helmut, N. Funk, *et al.*, “Tactile-conditioned diffusion policy for force-aware robotic manipulation,” *arXiv:2510.13324*, 2025.
- [29] A. Adeniji, Z. Chen, *et al.*, “Feel the force: Contact-driven learning from humans,” *preprint arXiv:2506.01944*, 2025.
- [30] H. Choi, Y. Hou, *et al.*, “In-the-wild compliant manipulation with UMI-FT,” *preprint arXiv:2601.09988*, 2026.
- [31] J. Huang, S. Wang, *et al.*, “Tactile-VLA: Unlocking vision-language-action model’s physical knowledge for tactile generalization,” *arXiv:2507.09160*, 2025.
- [32] B. Huang, J. Xu, *et al.*, “VT-Refine: Learning bimanual assembly with visuo-tactile feedback via simulation fine-tuning,” in *Conference on Robot Learning*, 2025.
- [33] C.-Y. Kuo, H. Shin, *et al.*, “Tracing energy flow: Learning tactile-based grasping force control to reduce slippage in dynamic object interaction,” *IEEE Robotics and Automation Letters*, 2025.
- [34] ROBOTIS, “Dynamixel XL430-W250-T,” <https://emanual.robotis.com/docs/en/dxl/x/xl430-w250/>, 2024, [Accessed: 08-17-2025].
- [35] A. Vaswani, N. Shazeer, *et al.*, “Attention is all you need,” *Advances in neural information processing systems*, 2017.
- [36] Y. Zhou, C. Barnes, *et al.*, “On the continuity of rotation representations in neural networks,” in *IEEE/CVF conference on computer vision and pattern recognition*, 2019.
- [37] A. Radford, J. W. Kim, *et al.*, “Learning transferable visual models from natural language supervision,” in *International Conference on Machine Learning*, 2021.

APPENDIX

A. Can RETAF replace gripper action prediction in the base policy?

We study whether RETAF can fully replace gripper force prediction by letting it jointly predict open/close and force. We compare the standard DP+RETAF setting with a variant where the base policy predicts only arm pose and RETAF predicts both open/close and force. As shown in Table IV, removing gripper action prediction from the base policy leads to a significant performance drop. We observe that without global visual observations, RETAF relies only on wrist images and tactile feedback and struggles to infer task progress and decide when to grasp. These results show that determine when to grasp and reactive force control serve distinct roles. While RETAF is effective at regulating force during contact, deciding when to close the gripper requires

global task context and cannot be reliably handled by RETAF alone.

TABLE IV: Ablation on removing gripper action prediction from the base policy.

Task	DP + RETA			DP w/o Gripper Action + RETA		
	Reach	Stable Grasp	Task Success	Reach	Stable Grasp	Task Success
Cherry Tomato	100%	90%	80%	100%	20%	0%
Liquid Transfer	70%	60%	60%	80%	0%	0%

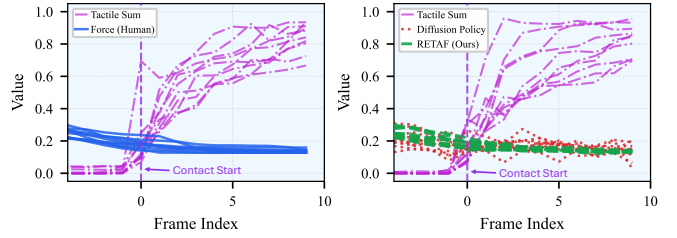


Fig. 10: Force and tactile signal evolution before and after contact during training (left) and rollouts (right). The tactile sum is min-max scaled to [0, 1], and force is scaled to [-1, 1], where values greater than 0 indicate the magnitude of grasping force. In human demonstrations, the gripper closes with relatively larger force before contact and then adjusts the force after contact based on visual and tactile feedback, resulting in characteristic force modulation. During rollouts, we compare force predictions from a Diffusion Policy and RETAF around contact. While the Diffusion Policy captures the overall trend, its predictions are noticeably noisier and less precise. In contrast, RETAF more closely reproduces the force modulation pattern observed in human demonstrations. Results are shown for 10 randomly selected trajectories from the cherry tomato picking task.

B. Force and Tactile Dynamics Around Contact

To investigate whether our policy captures the essential force-action coupling present in the expert demonstrations, we analyze the temporal correlation between sensed tactile signals and force adjustments on the representative cherry tomato picking task. This analysis is particularly critical around the moment of *initial contact*, where the transition from free motion to physical interaction requires immediate reactive force modulation. We visualize the evolution of force commands aligned with tactile feedback in both human demonstrations and policy rollouts (Fig. 10). In human demonstrations, we observe a distinct pattern where force is dynamically adjusted immediately following the onset of tactile signals. Comparing the policies, while the baseline captures the general trend, RETAF reproduces the reactive force modulation patterns observed in expert demonstrations with significantly higher fidelity. This suggests that the high-frequency Force Adaptation Policy in RETAF effectively learns the fine-grained dependency between tactile feedback and force regulation.

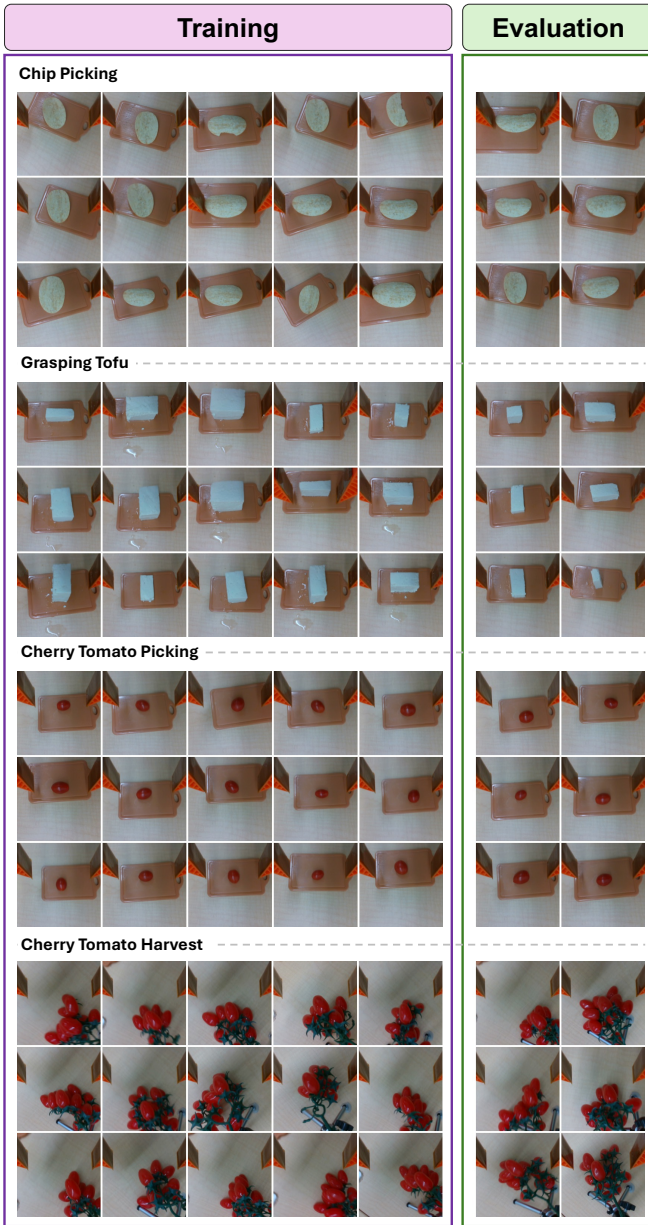


Fig. 11: Randomly selected gripper-view images captured before grasping during training and rollout across four tasks, illustrating the diversity of the training data. For each task, 15 training samples are shown, along with 6 randomly selected rollout frames. The liquid transfer task is not visualized, as the cup and tube are mounted on a fixed rig with largely identical gripper views.

C. Data Diversity and Rollout Comparison

In Fig. 11, we present randomly sampled gripper-view images captured before grasping from both the training dataset and evaluation rollouts. This visualization demonstrates the consistency of the data distribution between the training and evaluation phases. This ensures that the performance differences observed between our model and the baselines are attributable to policy capability under in-distribution conditions, rather than artifacts of domain shifts.